



HAL
open science

From conservative to reactive transport under diffusion-controlled conditions

Tristan Babey, Jean-Raynald De Dreuzy, Timothy R. Ginn

► **To cite this version:**

Tristan Babey, Jean-Raynald De Dreuzy, Timothy R. Ginn. From conservative to reactive transport under diffusion-controlled conditions . Water Resources Research, 2016, 52 (3), pp.3685-3700. 10.1002/2015WR018294 . insu-01308667

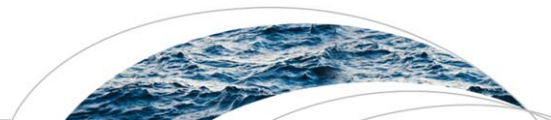
HAL Id: insu-01308667

<https://insu.hal.science/insu-01308667>

Submitted on 17 May 2016

HAL is a multi-disciplinary open access archive for the deposit and dissemination of scientific research documents, whether they are published or not. The documents may come from teaching and research institutions in France or abroad, or from public or private research centers.

L'archive ouverte pluridisciplinaire **HAL**, est destinée au dépôt et à la diffusion de documents scientifiques de niveau recherche, publiés ou non, émanant des établissements d'enseignement et de recherche français ou étrangers, des laboratoires publics ou privés.



RESEARCH ARTICLE

10.1002/2015WR018294

From conservative to reactive transport under diffusion-controlled conditions

Key Points:

- Simulation of nonlinear fluid-rock interactions under diffusive-controlled transport
- Derivation of concentration distributions from conservative transport by MRMT models
- Mono-component reactivity accurately estimated by parsimonious MRMT models

Correspondence to:

T. Babey,
tristan.babey@univ-rennes1.fr

Citation:

Babey, T., J.-R. de Dreuzy, and T. R. Ginn (2016), From conservative to reactive transport under diffusion-controlled conditions, *Water Resour. Res.*, 52, doi:10.1002/2015WR018294.

Received 28 OCT 2015

Accepted 16 APR 2016

Accepted article online 25 APR 2016

Tristan Babey¹, Jean-Raynald de Dreuzy¹, and Timothy R. Ginn²

¹Géosciences Rennes UMR CNRS 6118, Campus de Beaulieu, Université de Rennes 1, Rennes, France, ²Department of Civil and Environmental Engineering, Washington State University, Pullman, Washington, USA

Abstract We assess the possibility to use conservative transport information, such as that contained in transit time distributions, breakthrough curves and tracer tests, to predict nonlinear fluid-rock interactions in fracture/matrix or mobile/immobile conditions. Reference simulated data are given by conservative and reactive transport simulations in several diffusive porosity structures differing by their topological organization. Reactions includes nonlinear kinetically controlled dissolution and desorption. Effective Multi-Rate Mass Transfer models (MRMT) are calibrated solely on conservative transport information without pore topology information and provide concentration distributions on which effective reaction rates are estimated. Reference simulated reaction rates and effective reaction rates evaluated by MRMT are compared, as well as characteristic desorption and dissolution times. Although not exactly equal, these indicators remain very close whatever the porous structure, differing at most by 0.6% and 10% for desorption and dissolution. At early times, this close agreement arises from the fine characterization of the diffusive porosity close to the mobile zone that controls fast mobile-diffusive exchanges. At intermediate to late times, concentration gradients are strongly reduced by diffusion, and reactivity can be captured by a very limited number of rates. We conclude that effective models calibrated solely on conservative transport information like MRMT can accurately estimate monocomponent kinetically controlled nonlinear fluid-rock interactions. Their relevance might extend to more advanced biogeochemical reactions because of the good characterization of conservative concentration distributions, even by parsimonious models (e.g., MRMT with 3–5 rates). We propose a methodology to estimate reactive transport from conservative transport in mobile-immobile conditions.

1. Introduction

Transit time distributions obtained from conservative tracer testing are often used to predict chemically active transport [e.g., Becker and Shapiro, 2000; Charbeneau, 2006; Cirpka and Kitanidis, 2000; Ginn, 2001; Hadermann and Heer, 1996; Haggerty et al., 2001; LeBlanc et al., 1991; Ptak and Schmid, 1996]. Conservative transport models are then coupled to simple chemical models to investigate contaminant fate involving kinetically degrading compounds [Bohlke, 2002; Green et al., 2014; Heße et al., 2014], radioactively decaying species [Cvetkovic et al., 1999; Neretnieks, 1980], or sorbing solutes [Brusseau, 1992; Vereecken et al., 1999; Wels and Smith, 1994]. Reactivity can be straightforwardly inferred for linear approximation of reactivity, a case for which transport and chemical operators commute [Bahr and Rubin, 1987; Michalak and Kitanidis, 2000; Valocchi, 1990], as well as for more involved biogeochemical hysteretic cases through exposure time concepts [Ginn, 1999; Murphy and Ginn, 2000]. Similar approximations are also used at larger watershed and continental scales with more limited hydrological tracer information to constrain long-term fluid-rock interactions like weathering and dissolution rates [Clark and Fritz, 1997; Maher, 2010, 2011; Mukhopadhyay et al., 2014; Steefel and Maher, 2009; Yoo and Mudd, 2008]. However, for nonlinear sorption/desorption or precipitation/dissolution, bulk fluid-rock interactions cannot be inferred solely from transit time information and require some additional approximation of the concentration distribution [Attinger et al., 2009; Brusseau and Srivastava, 1997; Vereecken et al., 2002].

In some highly heterogeneous media, reactivity is controlled by the slow diffusion to the reactive sites located aside from the main advective channels, as in the case of fractured media in which solutes are quickly advected along the main connected fractures that account only for a minor part of the porosity and

slowly diffuse in the extensive but less connected fractures and in the large volume of surrounding rock [MacQuarrie and Mayer, 2005; Molson et al., 2012; Neretnieks, 1980; Steefel and Lichtner, 1994]. Similar behavior occurs in the case of inclusions of almost impervious structures in more pervious media and at smaller scales of complex dissolution patterns or clay aggregates [Luquot et al., 2014b; Murphy et al., 1997; Poonoosamy et al., 2015; Tyagi et al., 2013]. These slow diffusion processes have been identified as a source of failure of the advection-dispersion equation to model transport in heterogeneous formations motivating the development of alternative anomalous transport frameworks [Benson et al., 2000; Berkowitz et al., 2006; Berkowitz and Scher, 1998; Carrera et al., 1998; Haggerty and Gorelick, 1995]. Conceptually consistent with retardation and broad residence times, anomalous transport models have also been shown to model adequately field-scale breakthrough curves obtained from conservative tracer tests [e.g., Benson et al., 2001; Berkowitz and Scher, 1998; Haggerty et al., 2004; Le Borgne and Gouze, 2008; McKenna et al., 2001]. Once successfully calibrated on field data, they may offer a preferential way to assess the effect of slow transport processes on bulk reactivity. This has been demonstrated extensively for linear reaction processes using the commutativity of the transport and reaction operators [Haggerty and Gorelick, 1995; Margolin et al., 2003]. For nonlinear reactions, commutativity no longer holds and there is no guarantee that anomalous transport can be relevantly coupled to chemical reactions. Bulk reactivity is no longer determined by the sole time distribution at the basis of anomalous transport but also by the concentration distribution.

Despite this barrier, we investigate the capacity of anomalous transport to model nonlinear reactivity for the two following motivations. First, extending transport that appears anomalous due to diffusion to cases controlled by realistic chemical reactions is a major issue [Bolster et al., 2010; de Anna et al., 2011; de Dreuzy and Carrera, 2015]. Therefore we focus on effective pore scale modeling that honors genuine diffusion and nonlinear kinetically controlled reactions, unlike prior investigations [e.g., Willmann et al., 2010] which consider advection-controlled dispersion and equilibrium reactions. Second, one of the anomalous transport frameworks, the Multi-Rate Mass Transfer models (MRMT), has recently been shown numerically to conserve the concentration variance in the slow-diffusing zones (also called immobile or diffusive zones) for the specific 1D, 2D and 3D inclusion cases [de Dreuzy et al., 2013]. MRMT construction ensures only the conservation of the concentrations in the mobile zone and does not involve any constraint on the diffusive concentration distribution [Carrera et al., 1998; Haggerty and Gorelick, 1995; Willmann et al., 2008]. For 1D inclusions where analytical demonstration has been achieved, the conservation of immobile concentration variance is a byproduct of the mobile concentration conservation relation. Equivalent immobile MRMT concentrations are expressed as the product of the inclusion concentrations with orthogonal functions derived from the solution of the 1D diffusion equation [de Dreuzy et al., 2013]. This result is however limited to the concentration variance in layered inclusions. Nothing can be implied a priori for more complex structure or for chemical reactivity metrics other than concentration variance.

We thus evaluate the possibility to predict nonlinear kinetically controlled reactivity on the basis of conservative transport information in diffusion-dominated conditions, i.e., when access to the reactive sites is explicitly controlled by diffusion within poorly connected porosity structures ("diffusive zones"). Aside from the motivations mentioned above, the choice of MRMT is also instrumental as it gives a spatiotemporal distribution of concentrations in the immobile zones from conservative transport information. We simulate transport coupled to fluid-rock interactions in a broad range of diffusion-dominated porosity structures taken as ground-truth reference data, and compare it to MRMT equivalent models. While simple, our ground-truth model is an explicit porescale model that would require information about geological structures to be used in practical modeling. On the contrary, MRMT can be built solely from conservative transport information (e.g., breakthrough curves) and as such is commonly used as a practical model for passive tracers. Our purpose here is to continue to explore its use for reactive transport. We frame our results in a global methodology to approach chemical transport from conservative transport information. We eventually discuss its limitations and potential extensions to more general contexts.

2. Models and Methods

We present the reference reactive transport model with the transport processes, the diffusive porosity structures and the chemical reactions. We show how equivalent Multi-Rate Mass Transfer models (MRMT) are

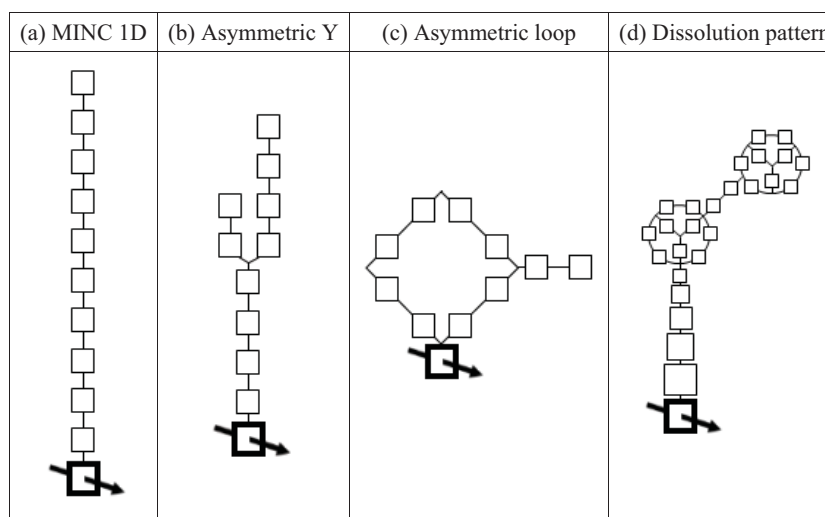


Figure 1. SINC structures used to evaluate the relevance of MRMT models for reactive transport. The mobile zone is represented by the thick black cell with the crossing arrow and the diffusive zones by the thin lined cells. From left to right, the diffusive porosity structures are (a) the classical 1-D Multiple Interacting Continua (MINC) model [Pruess and Narasimhan, 1985], (b) an asymmetric Y with a single junction, (c) an asymmetric loop, and (d) a structurally more involved pattern inspired by a dissolution feature in an oolitic limestone [Babey et al., 2015; Luquot et al., 2014a]. The area of the different cells is proportional to their porosity. The distance along the diffusive structure is to scale. The four structures have the same total porous volume, the same diffusive to mobile porosity ratio and the same quadratic mean distance of the diffusive zones to the mobile zone.

built from conservative transport information. We describe the synthetic experiments, criteria and numerical methods used to compare the reference and equivalent MRMT models.

2.1. Reference Reactive Transport Model

The reference reactive transport model is the Structured Interacting Continua (SINC) [Babey et al., 2015] taken as an extension of the Multiple Interacting Continua (MINC) introduced by Pruess and Narasimhan [1985]. In MINC, transport is mostly advective in one of the continua also called the mobile zone and diffusive across a finite number of continua connected in series to the mobile zone, here referred as the diffusive zones (Figure 1a). SINC is based on the same advectively controlled transport in the mobile zone interacting with a finite number of diffusive continua. These diffusive continua however differ by their connectivity (Figures 1b–1d). Organization may come from poorly connected fractures [Andersson et al., 2004; Davy et al., 2010] (Figure 1b), heterogeneous porosities [Gouze et al., 2008; Robinet et al., 2012] (Figure 1c), or dissolution patterns (Figure 1d) [Luquot et al., 2014b]. The four SINC structures of Figure 1 are the same used as references in Babey et al. [2015], except for their total diffusive porosity which is 10 times smaller. Because of their very distinct topologies, they are considered as characteristic of a large range of diffusive porosity structures. The finite number of diffusive zones would typically derive from a coarse description of the porosity or from a finite-difference discretization of diffusion within porous or fracture structures. The exchanges between the mobile and diffusive continua as well as the connectivity patterns are expected to determine the characteristic transport times, the mixing of water of different solute concentrations, the accessibility to the reactive sites and, eventually, the overall concentration distribution and dynamics.

In the SINC framework, aqueous species are transported by advection and dispersion along the mobile zone, and undergo diffusive-like exchanges (i.e., proportional to the difference of concentrations) between the mobile zone and some of the diffusion zones as well as between the diffusive zones. As in the MINC framework, the model is continuous along the mobile zone and discretized across the diffusive porosity. We assume that the transported aqueous species are reactive and interact by adsorption/desorption or precipitation/dissolution with the rock. Reactions are kinetically controlled. For the sake of simplicity, we assume that all stoichiometric coefficients are equal to one, and that the activities of all nonmineral species are equal to their concentrations. We do not consider feedbacks of reactivity on transport like induced porosity, diffusivity or velocity variations. Following classical multiporosity and reactive transport formalisms, the model then is formulated as [de Dieuleveult and Erhel, 2010; Steefel and Maher, 2009]:

$$\frac{\partial C}{\partial t} = \mathcal{L}(\mathbf{F}_m C) + \mathbf{A}C - R, \quad (1)$$

$$\frac{\partial S}{\partial t} = R. \quad (2)$$

$C(x, t) = [c_1(x, t) \ \dots \ c_{n+1}(x, t)]^T$ and $S(x, t) = [s_1(x, t) \ \dots \ s_{n+1}(x, t)]^T$ are the vectors of size $n+1$ made up of the aqueous and fixed (sorbed or precipitated) concentrations in the mobile zone for the first index ($c_1(x, t)$ and $s_1(x, t)$) and in the n diffusive zones for indices 2 to $n+1$. Both aqueous and fixed concentrations are taken as masses divided by the equivalent volume of fluid [ML^{-3}] (hereafter dimensions are given in dimension of mass [M], of length [L] and of time [T] [Yoo and Mudd, 2008]). x is the direction along the mobile zone with $0 \leq x \leq x_{\max}$. R is the reactive sink-source term further expressed in section 2.2. \mathbf{F}_m is the restriction matrix to the mobile zone:

$$\mathbf{F}_m(i, j) = \delta(i-1)\delta(j-1) \quad (3)$$

where δ is the Kronecker delta

$$\delta(i) = \begin{cases} 0 & \text{if } i \neq 0 \\ 1 & \text{if } i = 0 \end{cases}. \quad (4)$$

\mathcal{L} is the transport operator in the mobile zone

$$\mathcal{L}(c) = -\frac{q}{\phi_1} \frac{\partial c}{\partial x} + d_m \frac{\partial^2 c}{\partial x^2} \quad (5)$$

with q , ϕ_1 and d_m the Darcian flow [LT^{-1}], porosity and diffusive-dispersive coefficient [Bear, 1972; Scheidegger, 1954] [L^2T^{-1}] in the mobile zone.

The interaction matrix \mathbf{A} of size $(n+1, n+1)$ expresses the diffusive exchanges between the diffusive zones and with the mobile zone [Babey et al., 2015]. \mathbf{A} would typically be derived from a coarse discretization of the diffusive porosity. Its nonzero off-diagonal coefficients correspond to exchange rates [T^{-1}] between connected zones. Because \mathbf{A} integrates the porosity of the different zones, it is symmetrical only when all zones have the same porosity. It decomposes as

$$\mathbf{A} = -\Phi^{-1} \mathbf{M} \quad (6)$$

with \mathbf{M} the M-matrix expressing rates of exchanges of mass, and Φ the diagonal matrix made up of the porosities of the different zones ϕ_i :

$$\Phi(i, j) = \phi_i \delta(i-j). \quad (7)$$

2.2. Heterogeneous Reactions

We consider the two classical cases of nonlinear kinetically controlled Freundlich sorption and mineral dissolution. The Freundlich sorption isotherm has been widely used to describe the nonlinear, reversible adsorption of metals and organic compounds by soils [Fetter, 2008; Weber et al., 1991]. Under kinetic control, it is generally expressed as:

$$R_i(c_i, s_i) = \frac{1}{\tau_r} ((kc_i)^v - s_i) \quad (8)$$

where τ_r [T] is the characteristic reaction time, k is a sorption capacity constant and v is an exponent related to sorption intensity. Observed values of v are commonly smaller or equal to 1. We use $v=1/2$ (desorption of order 1/2) corresponding to a common value for metals [Adhikari and Singh, 2003; Paikaray et al., 2005]. In this specific case, k is of the dimension of a concentration [ML^{-3}].

For dissolution, we study the case of the kinetically controlled dissolution of a mineral AB into two aqueous species A and B of concentrations c_i^A and c_i^B . We assume that the initial and boundary conditions are such that at all times $c_i^A = c_i^B = c_i$ and $s_i^{AB} = s_i$. While restrictive, this assumption enhances the sensitivity of the reaction to the concentration distribution by maximizing the availability of the reactants and thus reactions

rates [de Simoni et al., 2005]. The reaction is expressed as [Appelo and Postma, 2005; Steefel and Maher, 2009]:

$$R_r(c_i, s_i) = \begin{cases} 0 & \text{if } s_i=0 \text{ and } \frac{c_i}{k} < 1, \\ \frac{k}{\tau_r} \left(\left(\frac{c_i}{k} \right)^2 - 1 \right) & \text{otherwise.} \end{cases} \quad (9)$$

τ_r [T] is the characteristic reaction time and k [ML^{-3}] is the square root of the solubility product. This dissolution reaction is of order 2. We choose consistent definitions for the reaction constant and characteristic time k and τ_r for desorption (equation (8)) and dissolution (equation (9)) because of their consistent dimensions and similar influence on reactivity (section 2.4). Finally, we underline that the kinetic control of the reactions precludes the use of the conservative component framework [de Simoni et al., 2007; Gramling et al., 2002; Rubin, 1983].

2.3. Equivalent MRMT Models

In the Multi-Rate Mass Transfer (MRMT) framework [Carrera et al., 1998; Haggerty and Gorelick, 1995], all the diffusive zones exchange exclusively with the mobile zone. Each diffusive zone is characterized by its porosity ϕ_i and its rate of exchange α_i [T^{-1}]. MRMT models can be expressed within the framework of SINC by imposing connections exclusively between the mobile and diffusive zones such that the exchange matrix of equation (6) writes:

$$\begin{cases} \mathbf{M}(i, j) = 0 & \text{for } i > 1, j > 1 \text{ and } i \neq j \\ \mathbf{M}(i, 1) = \mathbf{M}(1, i) = -\phi_i \alpha_{i-1} & \text{for } i > 1 \\ \mathbf{M}(i, i) = -\sum_{j \neq i} \mathbf{M}(i, j) \end{cases} \quad (10)$$

Following up the work of Haggerty and Gorelick [1995], the equivalence between SINC and MRMT models is defined via identification of the mobile concentrations for a passive tracer. Babey et al. [2015] have shown that any SINC model (i.e., whatever the connectivity pattern of the diffusive zones) is algebraically equivalent to a unique MRMT model with the same number of diffusive zones. This equivalent MRMT can be identified algebraically using a linear transformation of the SINC exchange matrix (equation (6)). We use this identification method to derive equivalent MRMT for each of the four SINC structures of Figure 1. Chemical reactions are then applied on the MRMT concentrations of the mobile and diffusive zones.

2.4. Synthetic Experiments

We simulate desorption and dissolution (equations (8) and (9)) in the four diffusive structures displayed on Figure 1. To ensure temporal responses of the same order of magnitude, the total porosity of the diffusive zones as well as the characteristic diffusion time τ_d are taken equal. τ_d is defined as the mean diffusive time from the diffusive zones to the mobile zone. Initially, sorbed or precipitated species are uniformly distributed in the domain with a concentration s^0 at chemical equilibrium with the fluid:

$$s_1(x, t=0) = \dots = s_{n+1}(x, t=0) = s^0 \quad (11)$$

$$R_1(x, t=0) = \dots = R_{n+1}(x, t=0) = 0. \quad (12)$$

“Pure water” (i.e., with a solute concentration equal to zero) is then continuously injected at the inlet of the mobile zone

$$c_1(x=0, t > 0) = 0. \quad (13)$$

Fixed elements are progressively desorbed or dissolved, and then transported throughout the domain until they reach the downstream adsorbing boundary condition:

$$c_1(x=X_{\max}, t) = 0. \quad (14)$$

Continuous chemical interaction with the rock is maintained during transport.

Focusing on the coupling of the physical and chemical processes, we fix the hydraulic parameters and investigate the relative influence of the chemical processes. The dispersion coefficient in the mobile zone is

Table 1. Transport, Reaction and Numerical Parameters Used for the Simulations of Section 3 With the Characteristic Diffusion Time τ_d and the Consecutive Distance Covered by Advection in the Mobile Zone $q\tau_d/\phi_1$ Taken as Temporal and Spatial Reference Scales^a

Parameter	Value
$\sum_{i=2}^{n+1} \phi_i/\phi_1$	10
$d_m/(\tau_d(q/\phi_1)^2)$	10^{-8}
$Da=\tau_d/\tau_r$	0.1; 1; 10
s^0/k	0.1; 1; 10
$x_{\max}/(q\tau_d/\phi_1)$	1.5×10^{-3}
$dx/(q\tau_d/\phi_1)$	3×10^{-5}
dt/τ_d	4×10^{-4}

^a $\sum_{i=2}^{n+1} \phi_i/\phi_1$ is the diffusive to mobile porosity ratio. $d_m/(\tau_d(q/\phi_1)^2)$ is the dimensionless dispersion in the mobile zone. $Da=\tau_d/\tau_r$ is the Damköhler number for the kinetically controlled Freundlich desorption and mineral dissolution. s^0/k is the dimensionless ratio of the initial concentration of sorbed species to the sorption capacity constant for desorption, and of the initial concentration of precipitated species to the square root of the solubility product for dissolution. x_{\max} is the extension of the simulation domain in the direction of the mobile zone, dx is the spatial step along the mobile zone and dt is the time step.

classically taken much smaller than the characteristic multi-domain diffusion induced by the mobile-immobile exchanges $(\tau_d(q/\phi_m)^2)$ and the ratio of the total diffusive to mobile porosity is taken much larger than one $(\sum_{i=2}^{n+1} \phi_i/\phi_1=10)$ [Carrera et al., 1998; Willmann et al., 2008]. For both the chosen desorption and dissolution processes (equations (8) and (9)), the key parameters are the ratio of the characteristic diffusion to reaction times τ_d/τ_r and the normalized initial concentration s^0/k . The ratio of characteristic times is generally called Damköhler number $Da=\tau_d/\tau_r$ [Steefel and Maher, 2009]. Results are also a function of the initial condition s^0/k because the chemical reactions are nonlinear. We investigate the effect of both these parameters over two orders of magnitude around 1 [0.1;10]. Model parameters and their values are synthesized in Table 1.

2.5. Comparison Criteria

We assess the ability of MRMT models to capture the mobilization rates through the five first moments of the aqueous concentration distribution taken over the whole domain (mobile and diffusive porosities)

$$m^j(C, t) = \int_{x=0}^{x_{\max}} \sum_{i=1}^{n+1} \phi_i [c_i(x, t)]^j dx \quad (15)$$

with j the order of the moment $j = 1, \dots, 5$. Complementary comparison is provided by the mobilization time t_m [T] defined as the time at which 95% of the total initial mass of fixed species have been mobilized, such that with $\eta=0.05$:

$$m(S, t=t_m)/m(S, t=0) = \eta \quad (16)$$

with

$$m(S, t) = \int_{x=0}^{x_{\max}} \sum_{i=1}^{n+1} \phi_i s_i(x, t) dx. \quad (17)$$

2.6. Numerical Methods

Finite-difference discretization of the advection-dispersion processes in the mobile zone, exchanges within the diffusive zones, and chemical reactions are sequentially coupled [de Dreuzy et al., 2013; Steefel and MacQuarrie, 1996]. Reaction rates are integrated with the fourth-order Runge-Kutta ode45 method of MATLAB [Shampine and Reichelt, 1997]. SINC implementation is validated against a set of diffusive structures strictly equivalent to Multiple Interacting Continua (MINC) taken as a discretization of 1D diffusion in an homogeneous layered inclusion (Figure 1a) [Babey et al., 2015]. Coupling between transport and reactivity is validated against PHREEQC on a single dual porosity structure ($n=1$) by using the STAGNANT functionality [Parkhurst and Appelo, 1999].

3. Results

Mobilization times and concentration moments in SINC and MRMT are compared as functions of diffusive zone structure, reaction type and reaction parameters. We assess the possibility to use parsimonious MRMT models (with only 1–5 rates) to estimate reaction rates.

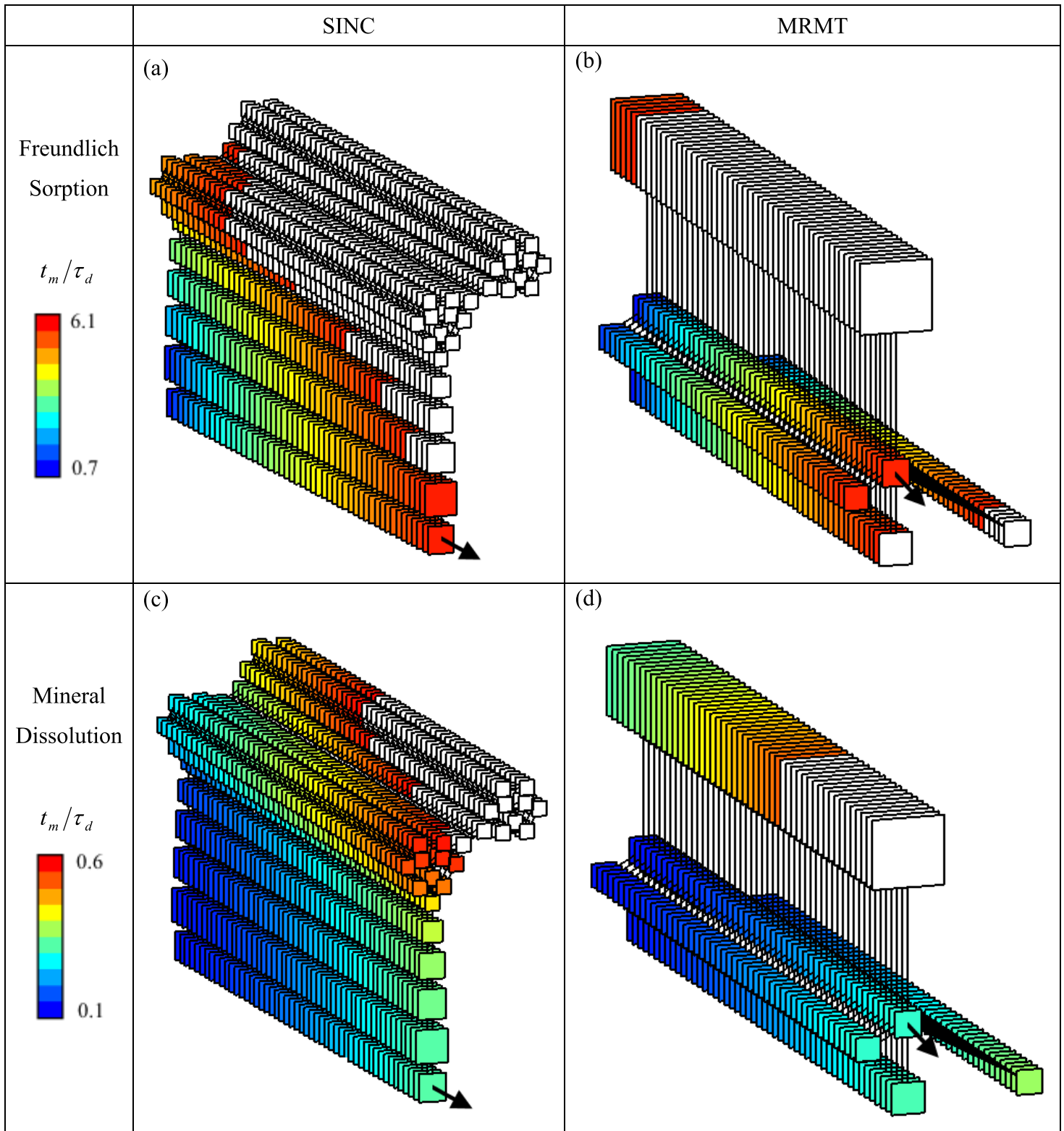


Figure 2. Mobilization times t_m/τ_d (section 2.5) for the Freundlich sorption (equation (9)) and the mineral dissolution (equation (10)) with $Da=\tau_d/\tau_r=10$ and $s^0/k=1$, for the SINC dissolution pattern (Figure 1d) and its equivalent MRMT model represented by its four zones with the largest porosities (out of 25), depicted as cross sections transverse to the mobile zone identified by the arrow. For the MRMT of the right column, the distances between the mobile and immobile zones are proportional to $\log(1/\alpha_i)$, and the porosities of the mobile and diffusive zones are proportional to the area of the cells.

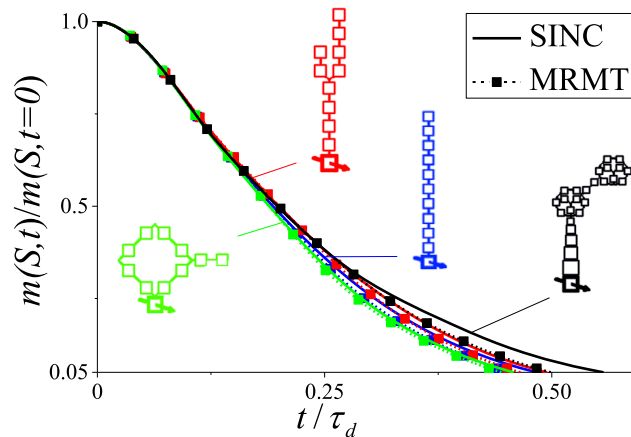


Figure 3. Remaining mass of mineral in the domain $m(S, t)$ for the four SINC structures of Figure 1 and their equivalent MRMT models. The dimensionless reaction parameters are $Da = \tau_d / \tau_r = 10$ and $s^0 / k = 1$.

3.1. Mobilization Times

The reaction front can be traced by the spatial repartition of the mobilization time t_m . Figure 2 represents t_m across the diffusive porosity and along the mobile zone for the SINC structure of Figure 1d and its equivalent MRMT model, for both the dissolution and the desorption cases. SINC and MRMT models both have 25 diffusive zones. In Figure 2, only the four MRMT diffusive zones with the largest porosities ϕ_i are represented as they account for more than 95% of the total diffusive porosity. The desorption and dissolution fronts progress quickly downstream the mobile zone but more slowly across the diffusive porosity.

MRMT zones with large exchange rates (small cells on Figure 2b) reproduce well the mobilization rates in the SINC zones close to the mobile porosity (Figure 2a). Both SINC and MRMT models display visually the same diffuse increase of the mobilization time in the few closest zones to the mobile zone. Diffusive zones away from the mobile zone in SINC are flushed much later (Figures 2a and 2c) like the zone with the smallest exchange rate for MRMT (largest cell more distant from the central mobile zones of Figures 2b and 2d). Mobilization times t_m for dissolution are intermediary between τ_r and τ_d ($0.1 \leq t_m / \tau_d \leq 0.6$) and about one order of magnitude smaller than mobilization times for desorption. For this parameterization, desorption is slower than dissolution because of its lower order (1/2) and its dependency on the sorbed species concentration.

The most apparent difference between SINC and MRMT on Figure 2 does not come from the mobilization time but from the nature of the discretization. All non-represented MRMT zones account for less than 5% of the overall diffusive porosity and are characteristic of extremely short exchange times. Nonetheless, diffusive zones next to the mobile porosity are well characterized and discretized by MRMT as they control fast

1	1	-2×10^{-3}	-2×10^{-3}	-9×10^{-4}	-4×10^{-3}
0.1	1	-6×10^{-4}	-6×10^{-4}	-3×10^{-4}	-1×10^{-3}
10	1	-3×10^{-3}	-2×10^{-3}	-1×10^{-3}	-6×10^{-3}
1	0.1	-3×10^{-3}	-2×10^{-3}	-2×10^{-3}	-6×10^{-3}
1	10	-8×10^{-4}	-7×10^{-4}	-3×10^{-4}	-2×10^{-3}
Da	s^0 / k	$(t_m^{MRMT} - t_m^{SINC}) / t_m^{SINC}$			

Figure 4. Relative differences on the mobilization time $(t_m^{MRMT} - t_m^{SINC}) / t_m^{SINC}$ between the four SINC models presented on Figure 1 and their equivalent MRMT models for the kinetically controlled Freundlich desorption (section 2.2). The dimensionless reaction parameters are the Damköhler number Da and the normalized initial concentration of fixed species s^0 / k .

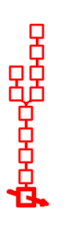
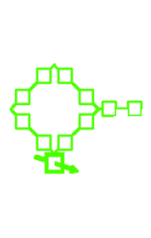
					
1	1	-2×10^{-3}	-2×10^{-3}	-6×10^{-4}	-5×10^{-3}
0.1	1	$< 10^{-5}$	$< 10^{-5}$	$< 10^{-5}$	4×10^{-5}
10	1	-6×10^{-2}	-6×10^{-2}	-3×10^{-2}	-1×10^{-1}
1	0.1	-3×10^{-2}	-3×10^{-2}	-1×10^{-2}	-6×10^{-2}
1	10	2×10^{-4}	3×10^{-4}	4×10^{-5}	7×10^{-4}
Da	s^0/k	$(t_m^{MRMT} - t_m^{SINC})/t_m^{SINC}$			

Figure 5. Relative differences on the mobilization time $(t_m^{MRMT} - t_m^{SINC})/t_m^{SINC}$ between the four SINC models presented on Figure 1 and their equivalent MRMT models for the kinetically controlled mineral dissolution (section 2.2). The dimensionless reaction parameters are the Damköhler number Da and the normalized initial concentration of fixed species s^0/k .

exchanges between the mobile and the diffusive zones. On the opposite, at late times, discretization of MRMT is extremely coarse. The late-time contribution to mobile-diffusive exchanges by the SINC porosity structure is represented by a single large lumped porosity zone in MRMT. This follows from the essence of diffusion. Late-time responses are smoothed out by diffusion and are dominated by more remote parts of the diffusive porosity. They do not need to be finely discretized and their contribution to mobile-diffusive exchanges can be represented by a single large lumped porosity zone. In synthetic terms, MRMT models discretize the exchanges with the diffusive porosity at early times and homogenize them at late times. Hence, the mobilization time in the large MRMT zone with the smallest exchange rate corresponds to an average value for the more remote zones of the SINC structure.

The accurate description of the early-time exchanges is confirmed by the close integrated desorbed and dissolved masses between SINC and MRMT models (Figure 3, lines for SINC and symbols for MRMT). MRMT models give observable differences only in the dissolution case and for the more complex diffusive structure of Figure 1d when more than 50% of the originally precipitated species have been dissolved. Still these differences remain small as shown by the relative difference in mobilization times between the SINC and MRMT models. Relative errors on the mobilization time t_m are commonly less than 1% with maximum values obtained for $Da=10$ and $s^0/k=1$, i.e., when the reaction becomes transport-limited. In this case errors increase from the better-connected asymmetric loop structure (0.1% for desorption (Figure 4), 3% for dissolution (Figure 5)) to the asymmetric Y and the MINC structures (0.3% and 6% each) and eventually to the less-connected dissolution pattern structure

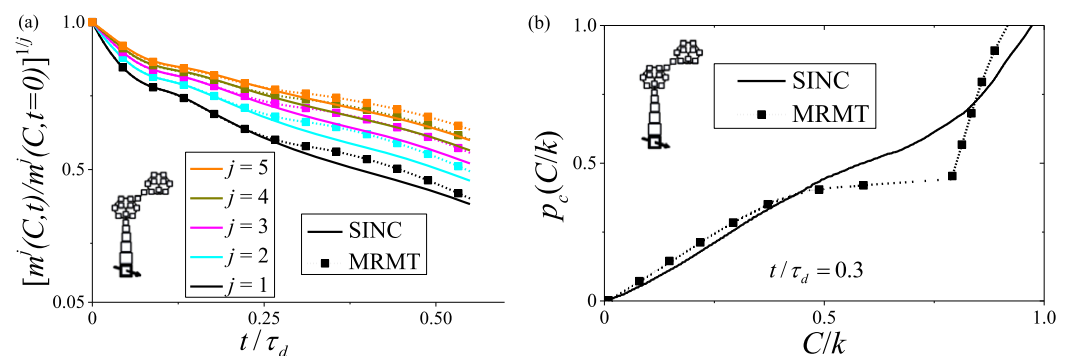


Figure 6. For the mineral dissolution with $Da=\tau_d/\tau_r=10$ and $s^0/k=1$: (a) Moments of the concentration distribution of the aqueous species $m^j(C, t)$ for the dissolution pattern SINC model (Figure 1d) and its equivalent MRMT model; (b) Cumulated concentration distribution of the aqueous species $p_c(C/k)$ at $t/\tau_d=0.3$ for the dissolution pattern SINC model (Figure 1d) and its equivalent MRMT model.

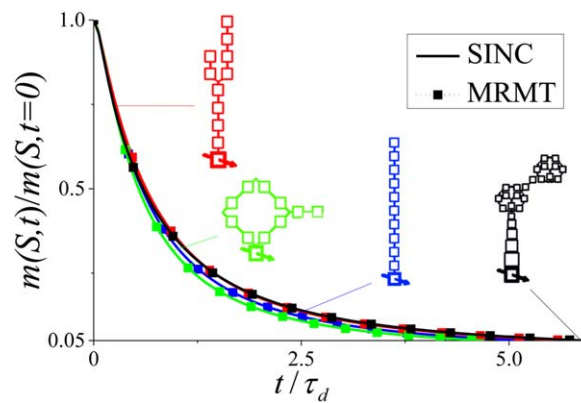


Figure 7. Remaining mass of sorbed species in the domain $m(S, t)$ for the four SINC structures of Figure 1 and their equivalent MRMT models. The dimensionless reaction parameters are $Da = \tau_d / \tau_r = 10$ and $s^0/k = 1$.

As they illustrate the effect of the MRMT discretization pattern displayed by Figure 2. Lower values of precipitated mass observed at intermediary times ($0.2 \leq t/\tau_d \leq 0.6$) on Figure 3 directly translate to higher values of the aqueous concentration moments (Figure 6a). A closer inspection of the distribution of solute concentrations taken over the entire domain at $t/\tau_d = 0.3$ (Figure 6b) shows important deviations at large concentration values ($C/k > 0.5$) characteristic of the remote diffusive zones where mineral is more slowly flushed. The largest lumped zone of the MRMT cannot fully capture the complex concentration patterns of the SINC structure. While the lumped representation of the complex SINC structure far from the mobile zone leads to accurate predictions for conservative transport, it gives some differences for reactive transport at intermediary times. At late times ($t/\tau_d \geq 0.6$), the strong homogenization effect of diffusion eventually dominates and reduces the differences. While qualitatively also present in the desorption case, deviations between SINC and MRMT are much more limited than in the dissolution case (Figures 7 and 8). Desorption is better matched than dissolution because it occurs more progressively and does not present the reaction rate discontinuity when the mineral vanishes.

The relevance of MRMT for reactive transport is consistent with its good characterization of the concentration distribution for conservative transport. By construction MRMT models reproduce the moments of the concentration distribution of order zero and one for a nonreactive tracer (conservation of the total porous volume and of the total mass of conservative solute respectively). MRMT models also reproduce the second moment of the concentration distribution for MINC diffusive structures as the one shown on Figure 1a [de Dreuzy *et al.*, 2013]. We check that it is also the case for the four studied SINC structures as shown for the dissolution pattern on Figure 9. Moments of order three and above are not equal, but remain very close.

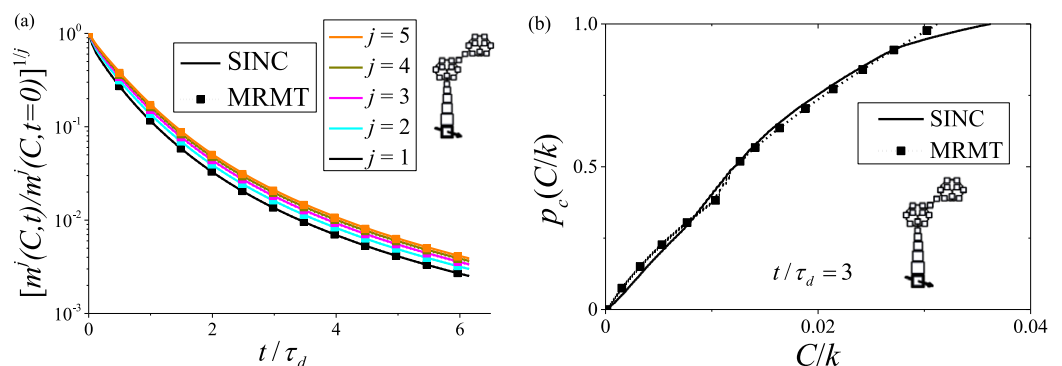


Figure 8. For the Freundlich desorption with $Da = \tau_d / \tau_r = 10$ and $s^0/k = 1$: (a) Moments of the concentration distribution of the aqueous species $m^j(C, t)$ for the dissolution pattern SINC model (Figure 1d) and its equivalent MRMT model; (b) Cumulated concentration distribution of the aqueous species $p_c(C/k)$ at $t/\tau_d = 3$ for the dissolution pattern SINC model (Figure 1d) and its equivalent MRMT model.

(0.6% and 10%). To summarize, errors by MRMT remain lower than 10% in all cases and decrease when mobilization times increase (i.e., slower reactions (smaller Da), larger initial amounts of fixed species (larger s^0/k), desorption instead of dissolution) as homogenization of concentrations by diffusion is more important and reduces the influence of porosity structures on bulk reactivity.

3.2. Concentration Distributions

The largest deviations occur in the SINC case of Figure 1d. Although limited, these differences are worth investigating as they illustrate the effect of the MRMT discretization pattern displayed by Figure 2.

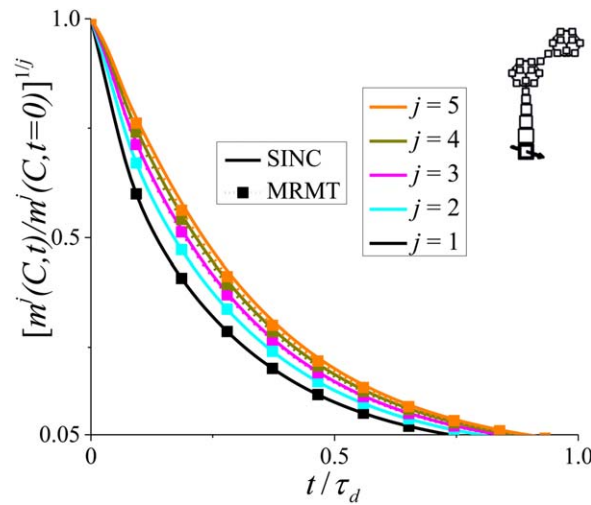


Figure 9. Moments of the concentration distribution $m^j(C, t)$ of a non-reactive tracer for the dissolution pattern SINC model (Figure 1d) and its equivalent MRMT model. The tracer is initially uniformly distributed in the domain and is flushed out by a continuous injection of a solution with a concentration equal to zero at the mobile inlet. The transport and numerical parameters used in the simulation are listed in Table 1.

Except in the extreme cases of complex diffusive porosity structures far away from the mobile zone, where errors can be as high as 10% on the mobilization time for dissolution, errors remain smaller than a few percent. As previously noted for conservative transport [Haggerty and Gorelick, 1995; Villiermaux, 1987], the relevance of MRMT models comes from their ability to accurately represent rapid exchanges with numerous exchange rates and from the homogenization nature of diffusion. The strong diffusive-induced homogenization is also reflected in the restricted dispersion of the precipitated and sorbed masses between the four SINC structures (Figures 3 and 7). All structures display close reaction rates. It is first and foremost the diffusive volume and the mean diffusion time to the mobile zone τ_d that determine the reactivity within the diffusive zones. The large geometrical and topological differences between the structures of

Figures 1a–1c do not induce significant differences in reactivity. Only very marked structures like the weak connections within the dissolution pattern (Figure 1d) have some limited impact on reactivity (Figure 3) as they restrain the access to some of the immobile zones and delay the dissolution within them.

3.3. Simplified MRMT Models

For conservative transport, SINC models are algebraically equivalent to MRMT models having the same number of zones [Babey et al., 2015]. It is precisely these equivalent MRMT models that have been used so far in this study. They have as many zones as the original SINC models. Approximate MRMT models with fewer zones can alternatively be built based on numerical flushing experiments of the diffusive zones [Babey et al., 2015]. The MRMT with a single zone or single rate ($n=1$) is the classical double porosity model with one mobile zone and one immobile zone [Warren et al., 1963]. With 2 exchange rates ($n=2$), it is the triple porosity model [e.g., Wu et al., 2004].

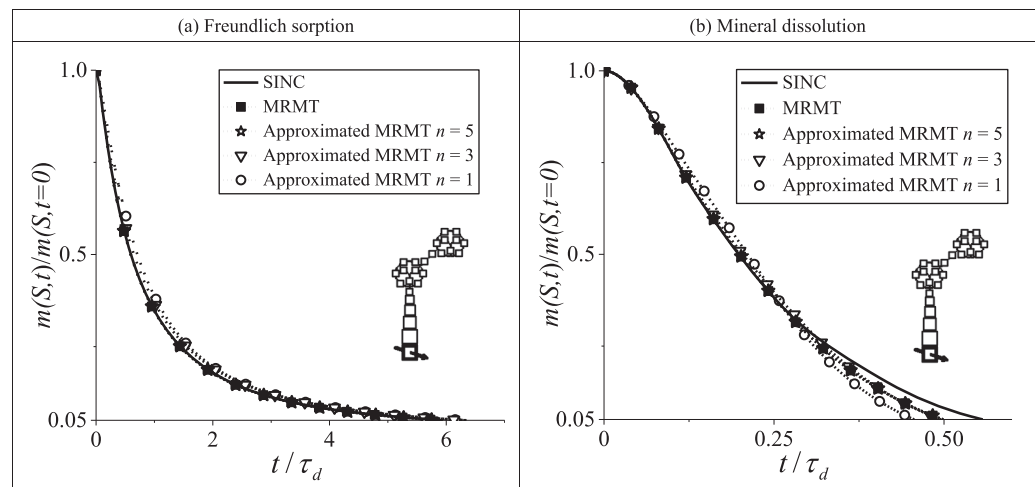


Figure 10. Remaining mass of (a) adsorbed species and (b) mineral in the domain $m(S, t)$ for the dissolution pattern SINC model (Figure 1d) and its equivalent MRMT model, either determined algebraically (section 2.3) or approximated with a limited number of n rates (section 3.3). The dimensionless reaction parameters are $Da = \tau_d / \tau_r = 10$ and $s^0 / k = 1$.

We assess the performances of these approached MRMT models according to their number of diffusive porosities (n) on the reactive transport experiment considered above, first on the remaining sorbed and precipitated masses (Figure 10). The double porosity model remains in the range of the full MRMT and reference SINC. Simplified MRMT models with increasing number of diffusive zones then rapidly converge to the behavior of the full MRMT. Quantitatively, for dissolution, $Da=10$ and $s^0/k=1$, errors on t_m drop down from a maximum of 20% for $n=1$ (double porosity model) to 11% for $n=3$ and 10% for $n=5$. Increasing the number of rates to the full MRMT ($n=25$) does not improve the approximation of t_m . Results are comparable for desorption where approximate values of t_m converge to the reference SINC value with relative differences of 7% ($n=1$), 6% ($n=3$) and 0.2% ($n=5$). The fast convergence comes from the dominance of the five first rates of the full MRMT that account for more than 95% of the diffusive porosity. The remaining rates characterize rapid exchanges that can be important only at very early times. It is consistent with the already discussed picture of diffusion where rapid interactions concern only the immediate volume next to the concentration injection, while longer-term exchanges are homogenized and can be represented by simple models with few parameters [Crank, 2002]. As for conservative transport (as shown in Haggerty and Gorelick [1995]), to increase the number of MRMT rates only marginally improves the approximation of short-term reactivity.

4. Discussion

The previous section has shown that MRMT models give good estimates of mono-component fluid-rock interactions over multiple complex porosity topologies. This consistency is fundamentally linked to the homogenization nature of diffusion and to the ability of MRMT models to capture concentration patterns beyond mass conservation. As the variability induced by the diffusive porosity structure is limited, even parsimonious MRMT models with a limited number of rates (3–5) can provide accurate predictions of reaction rates. Reactivity is primarily controlled by the ratio of diffusive to mobile porosity and by the quadratic mean transfer time to the diffusive zones. From a more applied point of view within the context of our present study, we propose the following methodology to approach reaction rates from breakthrough curves of conservative tracers. We eventually discuss the limitations and potential extensions of such approaches.

4.1. From Conservative Tracer Tests to Reactive Transport Estimates

We propose a three-step methodology to derive reactive MRMT simulations from conservative tracer test data. We choose MRMT among other anomalous transport frameworks like CTRW [Berkowitz *et al.*, 2006; Berkowitz and Scher, 1998], fADE [Benson *et al.*, 2000], or exposure-time mass transfer [Ginn, 2009], because it provides readily usable concentrations for reactions. Step one consists in verifying whether dispersion is diffusion-induced, for which our previous analysis pertains. Step two corresponds to the calibration of MRMT parameters upon the breakthrough curve (BTC) of a conservative tracer. In step three, reactions are simulated in the MRMT model.

4.1.1. Verification of Diffusion-Induced Dispersion Conditions

In this paper, we have considered diffusion-induced dispersion typical of fracture/matrix systems [Neretnieks, 1980; Roubinet *et al.*, 2013, 2010; Sudicky and Frind, 1982; Tang *et al.*, 1981; Zhou *et al.*, 2007] or mobile/immobile media [Golfier *et al.*, 2007; Haggerty *et al.*, 2004; Zinn *et al.*, 2004]. Transport variability also comes from local hydrodynamic effects [Bear, 1972] that contribute to the macro-dispersion typically observed in tracer experiments. As local dispersion has a similar expression as diffusion [Sánchez-Vila and Carrera, 2004], MRMT models could remain consistent as an intermediary between tracer experiments and reactivity estimates [Willmann *et al.*, 2010]. This should be analyzed and checked. If local dispersive effects require some specific treatment, their signature should be distinguished from diffusion. This could be done by varying the hydrodynamic parameters [Guiheneuf *et al.*, 2014] or the tracer diffusivity [Becker and Shapiro, 2000, 2003].

4.1.2. MRMT Model Calibration From BTC

MRMT parameters are calibrated from breakthrough curve information of a conservative tracer using any conventional procedure [e.g., Haggerty *et al.*, 2001]. Willmann *et al.* [2008] have also proposed a generic methodology where mobile and diffusive porosity parameters are identified successively. First mobile porosity ϕ_1 and diffusion-dispersion coefficient d_m (equation (5)) are obtained by fitting an advection-dispersion equation upon the first arrival and the peak of the BTC. Second, MRMT rates α and porosities ϕ (equation (10)) are calibrated by fitting the heavy tail of the BTC. The main difficulty lies in the potentially

large and irregular distributions of α and ϕ required to fit the BTC. It may be overcome by assuming an a priori density function $\phi(x)$. For example, *Haggerty et al.* [2000] have related the commonly observed power-law tailing of the breakthrough concentration c according to time t ($c \sim t^{-k}$) to the power-law density function $\phi \sim x^{k-3}$. However, complex diffusive porosity architectures are typically related to nonmonotonic density functions and nonparametric identification methods may have to be used [*Babey et al.*, 2015].

4.1.3. Using MRMT Concentrations for Reactions

Chemical reactions are applied on the MRMT concentrations of the mobile and diffusive zones. This can be achieved by using either the method presented in this article or alternatives like PHREEQC [*Parkhurst and Appelo*, 1999] that might give way to include more advanced reactive processes, as discussed in the next section. The model could be validated by comparing simulated and experimental breakthrough curves of a reactive species. It would typically be used to predict the apparent reduction of the reaction rates due to delayed access to the reactive surfaces, using for example spatially integrated reaction rates between an injection point and an observation point as an indicator of reaction advancement.

4.2. Extensions and Limitations of MRMT Approaches

While we study the overall capability of the MRMT modeling approach to handle kinetically controlled nonlinear reactions, it is important to keep in mind the limitations of this upscaling approach in field application. The parameters of the MRMT model are effective rate coefficients and capacities used to mimic collectively delayed transport associated with range of possible causes including anomalous dispersion, truly multi-rate diffusion, multiple sorption site types of different equilibria, and intermediate scale nonuniformities in advective transport. Determining the physical sense of MRMT parameters is a critical point to assess the predictive capabilities of MRMT models overall. However, in this paper we focus on whether MRMT can be used to predict reactivity in the first place under the conditions of the calibration. Investigation of the relations between MRMT fitted parameters and structural porosity features could be achieved through extensive numerical simulation of diverse SINC structures and by studying the algebraic transformation of SINC to MRMT.

Previous works have also shown the relevance of MRMT approaches to predict homogeneous and mixing-induced reactivity [*de Dreuzy et al.*, 2013; *Donado et al.*, 2009; *Willmann et al.*, 2010]. In addition to our results for heterogeneous reactions, this supports an extended validity of MRMT to a broader range of reactions. Fundamentally the very good characterization of the concentration distribution for a conservative solute extends to reactive solutes. Limitations would come from highly nonlinear reactions with strong positive feedbacks like auto-catalysis [*de Anna et al.*, 2010; *Gray and Scott*, 1983] or high initial concentration gradients in the diffusive porosity that cannot be recovered by MRMT [*de Dreuzy et al.*, 2013]. MRMT and beyond conservative tracers capture the physical constraint of reactivity as long as concentration patterns within the diffusive zones remain weakly correlated to the reaction process.

5. Conclusions

In this study we assess the possibility to use conservative transport information, like breakthrough curves from conservative tracer tests, to predict nonlinear fluid-rock interactions when reactivity is limited by slow diffusion to the reactive sites. For reference ground-truth data, we use the Structured INteracting Continua (SINC) framework where solute dispersion is primarily driven by exchanges between a fast, advective 1D mobile zone and an extensive diffusive porosity architecture coming from poorly connected fractures, low-permeability inclusions/matrix or dissolution patterns. The internal organization of the diffusive porosity and its connectivity to the mobile zone control the accessibility to the reactive sites. We select four reference SINC structures representative of different geological contexts and porous structure geometries. Reactions are taken as nonlinear kinetically controlled Freundlich sorption and mineral dissolution. The Multi-Rate Mass Transfer (MRMT) model is used as an intermediary between conservative transport information and reactive transport estimates. Reference and estimated reaction rates in SINC and their equivalent MRMT are compared for a flushing experiment.

Despite the noncommutativity of the reaction and transport operators for the nonlinear desorption and dissolution considered, MRMT models are shown to provide surprisingly close estimations of the bulk solubilization rates for both desorption and dissolution whatever the tested diffusive porosity structure. Errors are commonly less than 1% with maxima of 0.6% for sorption and 10% for dissolution obtained for fast

reactions, i.e., when the reaction becomes transport-limited. The first five moments of the aqueous reactant concentration distribution and the distributions themselves are similarly well approached. This is consistent with the very good characterization of the concentration distribution for conservative transport. Moments of order one and two for a passive tracer are equal in SINC and MRMT, and moments of higher order remain very close. The relevance of MRMT comes from its ability to accurately represent rapid exchanges between the mobile and diffusive porosities with numerous exchange rates, as well as from the homogenizing nature of diffusion itself. On one hand, diffusive zones next to the mobile porosity are well characterized and discretized by MRMT as they control short-term mobile-diffusive interactions. On the other hand, the coarse discretization of large-time exchanges reflects the homogenization operated by diffusion in the remote parts of the diffusive porosity. Deviations mainly occur in the case of complex diffusive porosity structures far away from the mobile zone where MRMT cannot capture persistent concentration gradients. While different, mobilization rates in the cases examined remain nonetheless close with differences smaller than a few percent or less.

Anomalous transport models derived solely from conservative transport information may thus be used to estimate nonlinear fluid-rock interactions when transport processes are dominated by slow diffusion to the reactive sites. Because conservative concentration distributions are well estimated, more advanced homogeneous and heterogeneous reactivities are likely to be also well captured. Additionally, we show that those models may not require an extensive parameterization, as parsimonious MRMT models with only a few diffusive zones remain highly effective. Dual-porosity models (MRMT with one diffusive zone) already give the proper order of magnitude of the mobilization times (maximum of 20% of error) and maximum precision is reached using a reduced five rates MRMT. For these reasons, we frame our results with a general methodology to estimate reaction rates from conservative transport information through anomalous transport models, using MRMT as an example. While highly effective for reaction under diffusion-controlled transport, the necessary extension to hydrodynamic-issued dispersion remains challenging.

Acknowledgments

The ANR is acknowledged for its funding through its project H2MNO4 under the number ANR-12-MONU-0012-01. This work was supported in part by NSF/EAR Project 1417495, "A practical upscaling of subsurface reactive transport." While the manuscript does not make use of experimental data, the Matlab numerical codes that have been used for the reactive transport simulations and MRMT identification are available by contacting the authors (tristan.babey@univ-rennes1.fr).

References

- Adhikari, T., and M. V. Singh (2003), Sorption characteristics of lead and cadmium in some soils of India, *Geoderma*, 114(1–2), 81–92, doi:10.1016/S0016-7061(02)00352-X.
- Andersson, P., J. Byegard, E.-L. Tullborg, T. Doe, J. Hermanson, and A. Winberg (2004), In situ tracer tests to determine retention properties of a block scale fracture network in granitic rock at the Aspo Hard Rock Laboratory, Sweden, *J. Contam. Hydrol.*, 70(3–4), 271–297.
- Appelo, C. A. J., and D. Postma (2005), *Geochemistry, Groundwater and Pollution*, 2nd ed., CRC Press, Leiden, Netherlands.
- Attinger, S., J. Dimitrova, and W. Kinzelbach (2009), Homogenization of the transport behavior of nonlinearly adsorbing pollutants in physically and chemically heterogeneous aquifers, *Adv. Water Resour.*, 32(5), 767–777, doi:10.1016/j.advwatres.2009.01.011.
- Babey, T., J. R. de Dreuzy, and C. Casenave (2015), Multi-Rate Mass Transfer (MRMT) models for general diffusive porosity structures, *Adv. Water Resour.*, 76, 146–156, doi:10.1016/j.advwatres.2014.12.006.
- Bahr, J. M., and J. Rubin (1987), Direct comparison of kinetic and local equilibrium formulations for solute transport affected by surface-reactions, *Water Resour. Res.*, 23(3), 438–452, doi:10.1029/WR023i003p00438.
- Bear, J. (1972), *Dynamics of Fluids in Porous Media*, Dover, N. Y.
- Becker, M. W., and A. M. Shapiro (2000), Tracer transport in fractured crystalline rock: Evidence of nondiffusive breakthrough tailing, *Water Resour. Res.*, 36(7), 1677–1686.
- Becker, M. W., and A. M. Shapiro (2003), Interpreting tracer breakthrough tailing from different forced-gradient tracer experiment configurations in fractured bedrock, *Water Resour. Res.*, 39(1), 1024, doi:10.1029/2001WR001190.
- Benson, D. A., S. W. Wheatcraft, and M. M. Meerschaert (2000), Application of a fractional advection-dispersion equation, *Water Resour. Res.*, 36(6), 1403–1412, doi:10.1029/2000WR900031.
- Benson, D. A., R. Schumer, M. M. Meerschaert, and S. W. Wheatcraft (2001), Fractional dispersion, Lévy motion, and the MADE tracer test, *Transp. Porous Media*, 42(1–2), 211–240, doi:10.1007/978-94-017-1278-1_11.
- Berkowitz, B., and H. Scher (1998), Theory of anomalous chemical transport in random fracture networks, *Phys. Rev. E*, 57(5), 5858–5869, doi:10.1103/PhysRevE.57.5858.
- Berkowitz, B., A. Cortis, M. Dentz, and H. Scher (2006), Modeling non-Fickian transport in geological formations as a continuous time random walk, *Rev. Geophys.*, 44, RG2003, doi:10.1029/2005RG000178.
- Bohlke, J. K. (2002), Groundwater recharge and agricultural contamination, *Hydrogeol. J.*, 10(1), 153–179, doi:10.1007/s10040-001-0183-3.
- Bolster, D., D. A. Benson, T. Le Borgne, and M. Dentz (2010), Anomalous mixing and reaction induced by superdiffusive nonlocal transport, *Phys. Rev. E*, 82(2), 021119.
- Brusseau, M. L. (1992), Transport of rate-limited sorbing solutes in heterogeneous porous media: Application of a one-dimensional multi-factor nonideality model to field data, *Water Resour. Res.*, 28(9), 2485–2497.
- Brusseau, M. L., and R. Srivastava (1997), Nonideal transport of reactive solutes in heterogeneous porous media 2. Quantitative analysis of the Borden natural-gradient field experiment, *J. Contam. Hydrol.*, 28(1–2), 115–155.
- Carrera, J., X. Sánchez-Vila, I. Benet, A. Medina, G. Galarza, and J. Guimerà (1998), On matrix diffusion: Formulations, solution methods and qualitative effects, *Hydrogeol. J.*, 6(1), 178–190, doi:10.1007/s100400050143.
- Charbeneau, R. J. (2006), *Groundwater Hydraulics and Pollutant Transport*, Waveland Press, Long Grove, Ill.
- Cirpka, O. A., and P. K. Kitanidis (2000), An advective-dispersive stream tube approach for the transfer of conservative-tracer data to reactive transport, *Water Resour. Res.*, 36(5), 1209–1220, doi:10.1029/1999WR900355.

- Clark, I. D., and P. Fritz (1997), *Environmental Isotopes in Hydrogeology*, CRC Press, N. Y.
- Crank, J. (2002), *The Mathematics of Diffusion*, Oxford Univ. Press, Oxford.
- Cvetkovic, V., J. O. Selroos, and H. Cheng (1999), Transport of reactive tracers in rock fractures, *J. Fluid Mech.*, 378, 335–356.
- Davy, P., R. Le Goc, C. Darcel, O. Bour, J. R. de Dreuzy, and R. Munier (2010), A likely universal model of fracture scaling and its consequence for crustal hydromechanics, *J. Geophys. Res.*, 115, B10411, doi:10.1029/2009JB007043.
- de Anna, P., F. Di Patti, D. Fanelli, A. J. McKane, and T. Dauxois (2010), Spatial model of autocatalytic reactions, *Phys. Rev. E*, 81(5), 056110.
- de Anna, P., T. Le Borgne, M. Dentz, D. Bolster, and P. Davy (2011), Anomalous kinetics in diffusion limited reactions linked to non-Gaussian concentration probability distribution function, *J. Chem. Phys.*, 135(17), 174104, doi:10.1063/1.3655895.
- de Dieuleveult, C., and J. Erhel (2010), A global approach to reactive transport: Application to the MoMas benchmark, *Comput. Geosci.*, 14(3), 451–464, doi:10.1007/s10596-009-9163-9.
- de Dreuzy, J. R., and J. Carrera (2015), On the validity of effective formulations for transport through heterogeneous porous media, *Hydrol. Earth Syst. Sci. Discuss.*, 12(11), 12,281–12,310, doi:10.5194/hessd-12-12281-2015.
- de Dreuzy, J. R., A. Rapaport, T. Babey, and J. Harmand (2013), Influence of porosity structures on mixing-induced reactivity at chemical equilibrium in mobile/immobile Multi-Rate Mass Transfer (MRMT) and Multiple INteracting Continua (MINC) models, *Water Resour. Res.*, 49, 8511–8530, doi:10.1002/2013WR013808.
- de Simoni, M., J. Carrera, X. Sanchez-Vila, and A. Guadagnini (2005), A procedure for the solution of multicomponent reactive transport problems, *Water Resour. Res.*, 41, W11410, doi:10.1029/2005WR004056.
- de Simoni, M., X. Sanchez-Vila, J. Carrera, and M. W. Saaltink (2007), A mixing ratios-based formulation for multicomponent reactive transport, *Water Resour. Res.*, 43, W07419, doi:10.1029/2006WR005256.
- Donado, L. D., X. Sanchez-Vila, M. Dentz, J. Carrera, and D. Bolster (2009), Multicomponent reactive transport in multicontinuum media, *Water Resour. Res.*, 45, W11402, doi:10.1029/2008WR006823.
- Fetter, C. W. (2008), *Contaminant Hydrogeology*, 2nd ed., Waveland Press Inc., N. Y.
- Ginn, T. R. (1999), On the distribution of multicomponent mixtures over generalized exposure time in subsurface flow and reactive transport: Foundations, and formulations for groundwater age, chemical heterogeneity, and biodegradation, *Water Resour. Res.*, 35(5), 1395–1407.
- Ginn, T. R. (2001), Stochastic-convective transport with nonlinear reactions and mixing: Finite streamtube ensemble formulation for multicomponent reaction systems with intra-streamtube dispersion, *J. Contam. Hydrol.*, 47(1), 1–28, doi:10.1016/S0169-7722(00)00167-4.
- Ginn, T. R. (2009), Generalization of the multirate basis for time convolution to unequal forward and reverse rates and connection to reactions with memory, *Water Resour. Res.*, 45, W12419, doi:10.1029/2009WR008320.
- Golfier, F., M. Quintard, F. Cherblanc, B. A. Zinn, and B. D. Wood (2007), Comparison of theory and experiment for solute transport in highly heterogeneous porous medium, *Adv. Water Resour.*, 30(11), 2235–2261, doi:10.1016/j.advwatres.2007.05.004.
- Gouze, P., Y. Melean, T. Le Borgne, M. Dentz, and J. Carrera (2008), Non-Fickian dispersion in porous media explained by heterogeneous microscale matrix diffusion, *Water Resour. Res.*, 44, W11416, doi:10.1029/2007WR006690.
- Gramling, C. M., C. F. Harvey, and L. C. Meigs (2002), Reactive transport in porous media: A comparison of model prediction with laboratory visualization, *Environ. Sci. Technol.*, 36(11), 2508–2514, doi:10.1021/es0157144.
- Gray, P., and S. K. Scott (1983), Autocatalytic reactions in the isothermal continuous, stirred-tank reactor: isolas and other forms of multistability, *Chem. Eng. Sci.*, 38, 29–43.
- Green, C. T., Y. Zhang, B. C. Jurgens, J. J. Starn, and M. K. Landon (2014), Accuracy of travel time distribution (TTD) models as affected by TTD complexity, observation errors, and model and tracer selection, *Water Resour. Res.*, 50, 6191–6213, doi:10.1002/2014WR015625.
- Guiheneuf, N., A. Boisson, O. Bour, B. Dewandel, J. Perrin, A. Dausse, M. Viossanges, S. Chandra, S. Ahmed, and J. C. Marechal (2014), Groundwater flows in weathered crystalline rocks: Impact of piezometric variations and depth-dependent fracture connectivity, *J. Hydrol.*, 511, 320–334, doi:10.1016/j.jhydrol.2014.01.061.
- Hadermann, J., and W. Heer (1996), The Grimsel (Switzerland) migration experiment: Integrating field experiments, laboratory investigations and modelling, *J. Contam. Hydrol.*, 21(1–4), 87–100.
- Haggerty, R., and S. M. Gorelick (1995), Multiple-rate mass transfer for modeling diffusion and surface reactions in media with pore-scale heterogeneity, *Water Resour. Res.*, 31(10), 2383–2400.
- Haggerty, R., S. A. McKenna, and L. C. Meigs (2000), On the late-time behavior of tracer test breakthrough curves, *Water Resour. Res.*, 36(12), 3467–3479, doi:10.1029/2000WR900214.
- Haggerty, R., S. W. Fleming, L. C. Meigs, and S. A. McKenna (2001), Tracer tests in a fractured dolomite 2. Analysis of mass transfer in single-well injection-withdrawal tests, *Water Resour. Res.*, 37(5), 1129–1142, doi:10.1029/2000WR900334.
- Haggerty, R., C. F. Harvey, C. F. von Schwerin, and L. C. Meigs (2004), What controls the apparent timescale of solute mass transfer in aquifers and soils? A comparison of experimental results, *Water Resour. Res.*, 40, W01510, doi:10.1029/2002WR001716.
- Heße, F., V. Prykhodko, S. Attinger, and M. Thullner (2014), Assessment of the impact of pore-scale mass-transfer restrictions on microbially-induced stable-isotope fractionation, *Adv. Water Resour.*, 74, 79–90, doi:10.1016/j.advwatres.2014.08.007.
- LeBlanc, D. R., S. P. Garabedian, K. M. Hess, L. W. Gelhar, R. D. Quadri, K. G. Stollenwerk, and Wood (1991), Large-scale natural gradient tracer test in sand and gravel, Cape Cod, Massachusetts, 1, Experimental design and observed tracer movement, *Water Resour. Res.*, 27(5), 895–910.
- Le Borgne, T., and P. Gouze (2008), Non-Fickian dispersion in porous media: 2. Model validation from measurements at different scales, *Water Resour. Res.*, 44, W06427, doi:10.1029/2007WR006279.
- Luquot, L., O. Rodriguez, and P. Gouze (2014a), Experimental characterization of porosity structure and transport property changes in limestone undergoing different dissolution regimes, *Transp. Porous Media*, 101(3), 507–532, doi:10.1007/s11242-013-0257-4.
- Luquot, L., T. S. Roetting, and J. Carrera (2014b), Characterization of flow parameters and evidence of pore clogging during limestone dissolution experiments, *Water Resour. Res.*, 50, 6305–6321, doi:10.1002/2013WR015193.
- MacQuarrie, K. T. B., and K. U. Mayer (2005), Reactive transport modeling in fractured rock: A state-of-the-science review, *Earth Sci. Rev.*, 72(3–4), 189–227, doi:10.1016/j.earscirev.2005.07.003.
- Maher, K. (2010), The dependence of chemical weathering rates on fluid residence time, *Earth Planet. Sci. Lett.*, 294(1–2), 101–110, doi:10.1016/j.epsl.2010.03.010.
- Maher, K. (2011), The role of fluid residence time and topographic scales in determining chemical fluxes from landscapes, *Earth Planet. Sci. Lett.*, 312(1–2), 48–58, doi:10.1016/j.epsl.2011.09.040.
- Margolin, G., M. Dentz, and B. Berkowitz (2003), Continuous time random walk and multirate mass transfer modeling of sorption, *Chem. Phys.*, 295(1), 71–80.
- McKenna, S. A., L. C. Meigs, and R. Haggerty (2001), Tracer tests in a fractured dolomite 3. Double-porosity, multiple-rate mass transfer processes in convergent flow tracer tests, *Water Resour. Res.*, 37(5), 1143–1154.

- Michalak, A. M., and P. K. Kitanidis (2000), Macroscopic behavior and random-walk particle tracking of kinetically sorbing solutes, *Water Resour. Res.*, *36*(8), 2133–2146, doi:10.1029/2000WR900109.
- Molson, J., M. Aubertin, and B. Bussière (2012), Reactive transport modelling of acid mine drainage within discretely fractured porous media: Plume evolution from a surface source zone, *Environ. Modell. Software*, *38*, 259–270, doi:10.1016/j.envsoft.2012.06.010.
- Mukhopadhyay, S., H. H. Liu, N. Spycher, and B. M. Kennedy (2014), Gaining insights into reactive fluid-fractured rock systems using the temporal moments of a tracer breakthrough curve, *J. Contam. Hydrol.*, *158*, 23–37, doi:10.1016/j.jconhyd.2013.12.003.
- Murphy, E. M., and T. R. Ginn (2000), Modeling microbial processes in porous media, *Hydrogeol. J.*, *8*, 142–158.
- Murphy, E. M., T. R. Ginn, A. Chilakapati, C. T. Resch, J. L. Phillips, T. W. Wietsma, and C. M. Spadoni (1997), The influence of physical heterogeneity on microbial degradation and distribution in porous media, *Water Resour. Res.*, *33*(5), 1087–1103.
- Neretnieks, I. (1980), Diffusion in the rock matrix: An important factor in radionuclides retardation?, *J. Geophys. Res.*, *85*(B8), 4379–4397, doi:10.1029/JB085iB08p04379.
- Paikaray, S., S. Banerjee, and S. Mukherji (2005), Sorption behavior of heavy metal pollutants onto shales and correlation with shale geochemistry, *Environ. Geol.*, *47*(8), 1162–1170, doi:10.1007/s00254-005-1262-x.
- Parkhurst, D. L., and C. A. J. Appelo (1999), User's guide to PHREEQC (version 2)—A computer program for speciation, batch-reaction, one-dimensional transport, and inverse geochemical calculations, Report 99-4259, U.S. Geol. Surv., Denver, Colo.
- Poonoosamy, J., G. Kosakowsld, L. R. Van Loon, and U. Mader (2015), Dissolution-precipitation processes in tank experiments for testing numerical models for reactive transport calculations: Experiments and modelling, *J. Contam. Hydrol.*, *177*, 1–17, doi:10.1016/j.jconhyd.2015.02.007.
- Pruess, K., and T. N. Narasimhan (1985), A practical method for modeling fluid and heat-flow in fractured porous-media, *SPEJ Soc. Pet. Eng. J.*, *25*(1), 14–26, doi:10.2118/10509-PA.
- Ptak, T., and G. Schmid (1996), Dual-tracer transport experiments in a physically and chemically heterogeneous porous aquifer: Effective transport parameters and spatial variability, *J. Hydrol.*, *183*(1-2), 117–138.
- Robinet, J.-C., P. Sardini, D. Coelho, J.-C. Parneix, D. Prêt, S. Sammartino, E. Boller, and S. Altmann (2012), Effects of mineral distribution at mesoscopic scale on solute diffusion in a clay-rich rock: Example of the Callovo-Oxfordian mudstone (Bure, France), *Water Resour. Res.*, *48*, W05554, doi:10.1029/2011WR011352.
- Roubinet, D., H. Liu, and J.-R. de Dreuzy (2010), A new particle-tracking approach to simulating transport in heterogeneous fractured porous media, *Water Resour. Res.*, *46*, W11507, doi:10.1029/2010WR009371.
- Roubinet, D., J.-R. de Dreuzy, and D. Tartakovsky (2013), Particle-tracking simulations of anomalous transport in hierarchically fractured rocks, *Comput. Geosci.*, *50*, 52–58, doi:10.1016/j.cageo.2012.07.032.
- Rubin, J. (1983), Transport of reacting solutes in porous-media—Relation between mathematical nature of problem formulation and chemical nature of reactions, *Water Resour. Res.*, *19*(5), 1231–1252, doi:10.1029/WR019i005p01231.
- Sánchez-Vila, X., and J. Carrera (2004), On the striking similarity between the moments of breakthrough curves for a heterogeneous medium and a homogeneous medium with a matrix diffusion term, *J. Hydrol.*, *294*(1-3), 164–175.
- Scheidegger, A. E. (1954), Statistical hydrodynamics in porous media, *J. Appl. Phys.*, *25*(8), 994–1001, doi:10.1063/1.1721815.
- Shampine, L. F., and M. W. Reichelt (1997), The MATLAB ODE Suite, *SIAM J. Sci. Comput.*, *18*(1), 1–22, doi:10.1137/S1064827594276424.
- Steeffel, C. I., and P. C. Lichtner (1994), Diffusion and reaction in rock matrix bordering a hyperalkaline fluid-filled fracture, *Geochim. Cosmochim. Acta*, *58*(17), 3595–3612, doi:10.1016/0016-7037(94)90152-X.
- Steeffel, C. I., and K. T. B. MacQuarrie (1996), Approaches to modeling of reactive transport in porous media, *Rev. Mineral.*, *34*(1), 85–129.
- Steeffel, C. I., and K. Maher (2009), Fluid-Rock Interaction: A Reactive Transport Approach, in *Thermodynamics and Kinetics of Water-Rock Interaction*, edited by E. H. Oelkers and J. Schott, pp. 485–532, Mineral. Soc. Am., Chantilly, Va, doi:10.2138/rmg.2009.70.11.
- Sudicky, E. A., and E. O. Frind (1982), Contaminant transport in fractured porous-media - analytical solutions for a system of parallel fractures, *Water Resour. Res.*, *18*(6), 1634–1642, doi:10.1029/WR018i006p01634.
- Tang, D. H., E. O. Frind, and E. A. Sudicky (1981), Contaminant transport in fractured porous-media - analytical solution for a single fracture, *Water Resour. Res.*, *17*(3), 555–564, doi:10.1029/WR017i003p00555.
- Tyagi, M., T. Gimmi, and S. V. Churakov (2013), Multi-scale micro-structure generation strategy for up-scaling transport in clays, *Adv. Water Resour.*, *59*, 181–195, doi:10.1016/j.advwatres.2013.06.002.
- Valocchi, A. J. (1990), Use of temporal moment analysis to study reactive solute transport in aggregated porous-media, *Geoderma*, *46*(1-3), 233–247.
- Vereecken, H., U. Jaekel, O. Esser, and O. Nitzsche (1999), Solute analysis of bromide, uranin and LiCl using breakthrough curves from aquifer sediment, *J. Contam. Hydrol.*, *39*, 7–34.
- Vereecken, H., U. Jaekel, and H. Schwarze (2002), Analysis of the long-term behavior of solute transport with nonlinear equilibrium sorption using breakthrough curves and temporal moments, *J. Contam. Hydrol.*, *56*(3-4), 271–294.
- Villermaux, J. (1987), Chemical-engineering approach to dynamic modeling of linear chromatography - a flexible method for representing complex phenomena from simple concepts, *J. Chromatogr.*, *406*, 11–26, doi:10.1016/s0021-9673(00)94014-7.
- Warren, J. E., P. J. Root, and M. Aime (1963), The behavior of naturally fractured reservoirs, *Soc. Pet. Eng. J.*, *3*(3), 245–255, doi:10.2118/426-PA.
- Weber, W. J., P. M. McGinley, and L. E. Katz (1991), Sorption phenomena in subsurface systems: concepts, models and effects on contaminant fate and transport, *Water Res.*, *25*(5), 499–528.
- Wels, C., and L. Smith (1994), Retardation of sorbing solutes in fractured media, *Water Resour. Res.*, *30*(9), 2547–2563.
- Willmann, M., J. Carrera, and X. Sanchez-Vila (2008), Transport upscaling in heterogeneous aquifers: What physical parameters control memory functions?, *Water Resour. Res.*, *44*, W12437, doi:10.1029/2007WR006531.
- Willmann, M., J. Carrera, X. Sanchez-Vila, O. Silva, and M. Dentz (2010), Coupling of mass transfer and reactive transport for nonlinear reactions in heterogeneous media, *Water Resour. Res.*, *46*, W07512, doi:10.1029/2009WR007739.
- Wu, Y. S., H. H. Liu, and G. S. Bodvarsson (2004), A triple-continuum approach for modeling flow and transport processes in fractured rock, *J. Contam. Hydrol.*, *73*(1-4), 145–179, doi:10.1016/j.jconhyd.2004.01.002.
- Yoo, K., and S. M. Mudd (2008), Discrepancy between mineral residence time and soil age: Implications for the interpretation of chemical weathering rates, *Geology*, *36*(1), 35–38, doi:10.1130/g24285a.1.
- Zhou, Q. L., H. H. Liu, F. J. Molz, Y. Q. Zhang, and G. S. Bodvarsson (2007), Field-scale effective matrix diffusion coefficient for fractured rock: Results from literature survey, *J. Contam. Hydrol.*, *93*(1-4), 161–187.
- Zinn, B., L. C. Meigs, C. F. Harvey, R. Haggerty, W. J. Peplinski, and C. F. Von Schwerin (2004), Experimental visualization of solute transport and mass transfer processes in two-dimensional conductivity fields with connected regions of high conductivity, *Environ. Sci. Technol.*, *38*(14), 3916–3926, doi:10.1021/es034958g.